Mustansiriyah Journal of Pure and Applied Sciences, Print ISSN: 2957-9910. Online ISSN: 2957-9929, Vol. 4, No. 3, 2026, Pages 119-134
DOI: 10.47831/mjpas.v4i3.464

MJPAS

MUSTANSIRIYAH JOURNAL OF PURE AND APPLIED SCIENCES

Journal homepage:
https://mjpas.uomustansiriyah.edu.iq/index.php/mjpas

RESEARCH ARTICLE - MATHEMATICS

A Perturbation Iteration Algorithm-Based Semi-Analytical Blood Flow Model for the Jeffrey Hamel

Ali Juwaiad Aswad Al-Maliki

Ministry of Education. Open Educational College, Al-Qurna Branch

E-mail: alaligwaed@gmail.com

Article Info.

Article history:

Received
26 June 2025

Accepted
9 September 2025

Publishing
30 September 2026

Abstract

This study presents an enhanced approach for solving the magneto- hydrodynamic nonlinear Jeffrey-Hamel (MHD-JHF) problem, modeling human arterial blood flow, using a hybrid metaheuristic combining Particle Swarm Optimization (PSO) and the Perturbation Iteration Algorithm (PIA). The model is formulated from third-order ordinary differential equations derived from the nonlinear MHD partial differential equations of Jeffrey-Hamel flow. Optimal artificial neural network weights are obtained by minimizing the fitness function through the PSO-PIA algorithm. The proposed method is evaluated across four MHD-JHF scenarios, considering different Reynolds numbers and channel angles. Numerical results demonstrate excellent agreement with reference solutions and highlight the importance of accurately characterizing arterial blood flow. Statistical analyses based on multiple performance metrics confirm the method's accuracy, efficiency, and reliability. The framework offers potential for future extension to related problems in science and engineering applications.

The official journal published by the College of Education at Mustansiriyah University

Keywords: Blood Flow, Artificial Neural Networks, Hybrid Optimization, Particle Swarm Optimization, Nonlinear PDEs, Magneto-Hydrodynamics, Perturbation Iteration Algorithm (PIA 1,1), Jeffrey-Hamel Flow, Reynolds Number

1.Introduction

In a wide range of scientific and engineering applications, one of the most significant phenomena is the internal flow between two divergent or convergent plates. Over the years, many researchers have focused on the two-dimensional incompressible flow between inclined plates, commonly referred to as Jeffrey-Hamel (JHF) flow. This problem has attracted considerable attention due to its importance in both theoretical studies and practical applications, such as the design of systems that optimize thermal management and fluid transport. Several analytical and numerical methods have been developed to approximate solutions for the Jeffrey-Hamel flow. Among these are the Differential Transform Method (DTM), Modified Sumudu Transform Method, Duanrach Approach (DRA), Adomian Decomposition Method, Traveling Wave Transformation Method, Homotopy Analysis Method (HAM), and Perturbation Iteration Algorithm (PIA). Patel and Meher [2] examined the magnetohydrodynamic (MHD) JHF problem using DTM in the presence of a magnetic field. Ramakanta and Patel [3] applied DTM to study MHD JHF flow of Cu-water nanofluid between two smooth rectangular walls under a transverse magnetic field. Salim Hamrelaine [4] solved the MHD Jeffrey-Hamel model using the homotopy perturbation method, while Marinca and Ene [5] investigated the temperature effects on MHD JHF flow using the Optimal Homotopy Perturbation Method (OHPM). Puneet [6] applied PHAM to obtain several MHD JHF solutions, and Dongochia et al. [7] used DRA to examine MHD nanofluid flow and heat transfer in a porous channel under thermal radiation. Asad and Faisal [8] analyzed MHD JHF flow in the presence of thermal effects using Spectral HAM, while Singh and Rashidi [9] employed a hybrid computational technique for JHF flow in non-parallel walls. These studies consistently examined the influence of Reynolds number, magnetic field, and other physical parameters on fluid flow, with the goal of achieving close agreement between analytical and numerical results [10]. To address these challenges, the Perturbation Iteration Algorithm PIA(1,1), especially PIA(1,1), has proven effective for obtaining analytical approximations of complex nonlinear problems. Previous research has successfully applied PIA(1,1) to rotating MHD viscous flows, heat transfer between porous and stretched surfaces, and Jeffrey-Hamel flow with nanoparticles in high magnetic fields [11]. The main objective of this work is to find an analytical approximation solution for the nonlinear problem describing incompressible viscous Jeffrey-Hamel flow. PIA is used in this study due to its iterative algorithm, which is structured based on the order of derivatives in Taylor expansions n_2

and the number of terms in the perturbation expansion n_1, referred to as PIA $(n_1, n_2), n_1, n_2 = 1,2, ...$ P IA(n_1, n_2),... [12]. The PIA(1,1) configuration is specifically investigated to ensure the convergence of the approximation series while reducing computational effort and maintaining high accuracy. Additionally, understanding the fluid mechanics of human arterial blood flow has important biomedical applications. Previous studies have examined the interaction of thermophoresis and Brownian motion on blood-based Casson nanofluid dynamics over nonlinearly expanding surfaces [6]. This research applies the Jeffrey-Hamel framework to model human arterial blood flow, providing insights for both biomedical engineering and heat transfer applications, as illustrated in Fig. 1.

Figure 1: The flow of blood in the human artery

A major threat to cardiovascular health, stenosis refers to the abnormal narrowing of a blood vessel, which often leads to reduced blood flow and increases the risk of serious complications, including heart attacks and strokes. Several factors contribute to the formation of stenotic arteries. As illustrated in Fig. 2, the blood flow is assumed to be incompressible and two-dimensional, behaving as a homogeneous Newtonian fluid within a stenosed artery of length L0/2 and width 2R0. The radial axis (r-axis) is defined perpendicular to the direction of flow, while the coordinate system is oriented such that the fluid moves along the (x-axis). The influence of geometric irregularities, whose profile is described as in [4], on the flow behavior is then investigated to understand how stenosis affects the velocity and pressure distribution within the artery

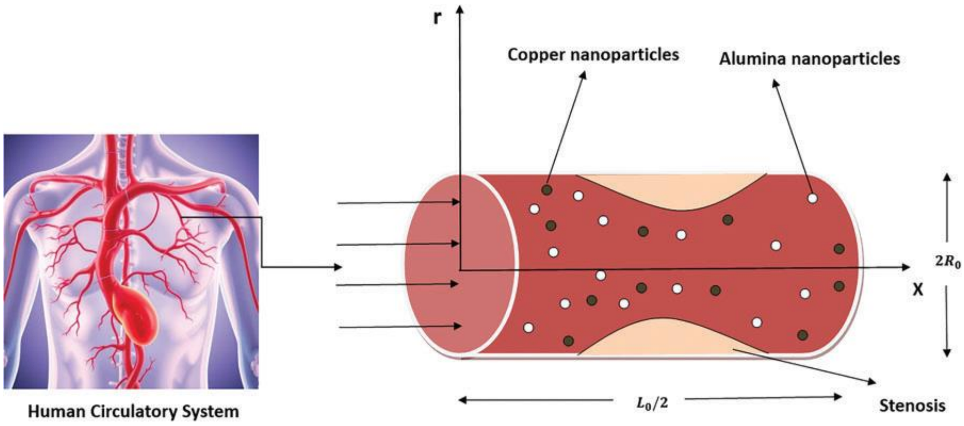

Figure 2: A physical illustration of the stenosed artery containing nanoparticles of copper and alumina

2- Mathematical Formulation

As seen in Figure 1, consider the continuous two-dimensional flow of an incompressible conductive viscous fluid between two rigid plane walls intersecting at angle $2a$. Here, it is assumed that the velocity depends only on r and h and is entirely radial. The Navies-Stokes equation and the continuity equation in polar coordinates are [11]:

Continuity equation:

$$\frac{\partial u_r(r,\theta)}{\partial r}+\frac{1}{r}u_r(r,\theta)=0, \tag{1}$$

Radial momentum equation:

$$-\mathrm{u_r}(\mathrm{r},\theta)\frac{\partial \mathrm{u_r}(\mathrm{r},\theta)}{\partial \mathrm{r}}-\frac{1}{\rho}\,\frac{\partial \mathrm{p}}{\partial \mathrm{r}}+\nu\left[\frac{\partial^2\mathrm{u_r}(\mathrm{r},\theta)}{\partial \mathrm{r}^2}+\frac{1}{\mathrm{r}}\,\frac{\partial \mathrm{u_r}(\mathrm{r},\theta)}{\partial \mathrm{r}}+\frac{1}{\mathrm{r}^2}\frac{\partial^2\mathrm{u_r}(\mathrm{r},\theta)}{\partial\theta^2}-\frac{\mathrm{u_r}(\mathrm{r},\theta)}{\mathrm{r}^2}\right]=0, \tag{2}$$

Tangential momentum equation:

$$-\frac{1}{p_r}\frac{\partial P}{\partial \theta}+\frac{2\,v}{r^2}\cdot\frac{\partial u_r(r,\theta)}{\partial \theta}=0, \tag{3}$$

This equation uses the symbols u(r) for radial velocity, p for pressure, V for kinematic viscosity, and p_r for fluid density. The equation that results from using dimensionless parameters in Eq (1) is as follows:[13]

$$\mathrm{u_r}=\mathrm{U_r},\quad \frac{\partial \mathrm{u_r}}{\partial\theta}=0 \quad \text{at} \quad \theta=0,$$
$$u_r=0,\quad at \quad \theta=\varphi, \tag{4}$$

As a result, we will begin by deriving the equations using non-dimensional transformations to convert them into a simple equation that can be solved analytically.

$$-\frac{\partial^2 u_r}{\partial\theta\partial r}-u_r\frac{\partial^2 u_r}{\partial\theta\partial r}-\frac{1}{\rho}\frac{\partial^2 p}{\partial\theta\partial r}+v\left[\frac{\partial^3 u_r}{\partial\theta\partial r^2}+\frac{1}{r}\,\frac{\partial^2 u_r}{\partial\theta\partial r}+\frac{1}{r^2}\frac{\partial^3 u_r}{\partial\theta^3}-\frac{1}{r^2}\frac{\partial u_r}{\partial\theta}\right]=0, \tag{5}$$

$$-\frac{1}{\rho}\frac{\partial^2 P}{\partial\theta\partial r}+\frac{1}{\rho r}\frac{\partial P}{\partial\theta}+v\left[\frac{2}{r}\frac{\partial^2 u_r}{\partial\theta\partial r}-\frac{4}{r^2}\frac{\partial u_r}{\partial\theta}\right]=0, \tag{6}$$

By subtracting the two equations (5) from (6), we obtain

$$-\frac{\partial^2 u_r}{\partial\theta\partial r}-u_{\dot r}\frac{\partial^2 u_r}{\partial\theta\partial r}-\frac{1}{\rho\dot r}\frac{\partial P}{\partial\dot\theta}+v\left[\frac{\partial^3 u_r}{\partial\theta\partial r^2}-\frac{1}{r}\,\frac{\partial^2 u_r}{\partial\theta\partial r}+\frac{1}{r^2}\frac{\partial^3 u_r}{\partial\theta^3}+\frac{3}{r^2}\frac{\partial u_r}{\partial\theta}\right]=0, \tag{7}$$

by integrating both sides with respect to r for continuity equation (1) in the form

$$f(\dot\theta)=ru_r(r,\theta), \tag{8}$$

the dimensionliss variables with the Equation (4), can eliminate all dimensions from the issue.

$$G(\eta)=\frac{f(\theta)}{rU_r},\qquad \delta=rU_r,\qquad \eta=\frac{\theta}{\varphi},\qquad u_r(r,\theta)=\frac{\delta}{r}\,G(\eta),$$

Equation (8) allows us to determine the necessary derivatives.

$$\frac{\partial u_r}{\partial\theta}=\frac{\delta}{r\varphi}\,\frac{dG(\eta)}{d\eta},\qquad \frac{\partial^3 u_r}{\partial\theta^3}=\frac{\delta}{\varphi^3 r}\,\frac{d^3G(\eta)}{d\eta^3},\qquad \frac{\partial^3 u_r}{\partial r^2\partial\theta}=\frac{2\delta}{\varphi r^3}\frac{dG(\eta)}{d\eta},$$

$$\frac{\partial u_r}{\partial r}=\frac{-\delta}{r^2}\,G(\eta),\qquad \frac{\partial^2 u_r}{\partial r\partial\theta}=\frac{-\delta}{\varphi r^2}\,\frac{dG(\eta)}{d\eta},\qquad \frac{\partial^2 u_r}{\partial r^2}=\frac{2\delta}{r^3}\,G(\eta)\,,$$

Now, by taking the aforementioned derivative and replacing it in equation (7), we obtain (7).

$$-\frac{2\delta^2}{\varphi r^3}G(\eta)\frac{dG(\eta)}{d\eta}-v\left[\frac{\delta}{\varphi^3 r^3}\frac{d^3G(\eta)}{d\eta^3}+\frac{4\delta}{\varphi r^3}\frac{dG(\eta)}{d\eta}\right]=0, \tag{9}$$

Using the hypothesis $R_e = \frac{\delta\varphi}{v}$ we multiply both sides of the equation by $\frac{\varphi^2}{v} \neq 0$, and by making them simpler, we get the following form

$$\frac{d^3G(\eta)}{d\eta^3}+2\varphi R_e G\,(\eta)\frac{dG(\eta)}{d\eta}+4\varphi^2\frac{dE(\eta)}{d\eta}=0, \tag{10}$$

The boundary condition of the problem dimensionless are

$$G(0)=1\quad,\qquad \frac{dG(0)}{d\eta}=0\quad,\qquad G(1)=0, \tag{11}$$

can classified to two cases as:

- Divergent Channel : $G > 0$, $U_r > 0$,
- Convergent Channel : $G < 0$, $U_r < 0$,

The values of the skin friction coefficient can be obtained by using [14]

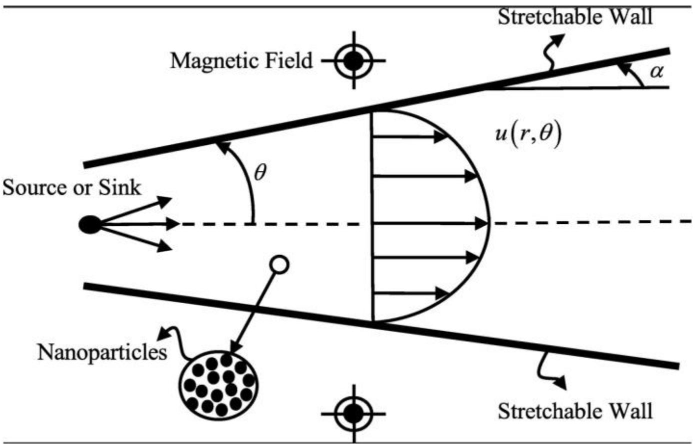

Figure 3: The geometry of the MHD Jeffery – Hamel flow.

3- Application of the Jeffery-Hamel Flow Problem.

The steps of the PIA(1,1) algorithm's application to the nonlinear differential equation to get an analytical approximate solution [10] can be shown as follows.;

$$\frac{d^3G(\eta)}{d\eta^3}+\varepsilon\left[2\varphi R_e E\,(\eta)\frac{dG(\eta)}{d\eta}+4\varphi^2\frac{dG(\eta)}{d\eta}\right]=0, \tag{12}$$

subjectboundary condition are:

$$G(0)=1\,,\qquad \frac{dG(0)}{d\eta}=0,\qquad G(1)=0, \tag{13}$$

the problem of the auxiliary perturbation parameter ε are

$$\mathrm{D}\left(\mathrm{G}(\eta),\frac{dG(\eta)}{d\eta},\frac{d^3G(\eta)}{d\eta^3},\epsilon\right)=\frac{d^3G(\eta)}{d\eta^3}+\epsilon\left[2\varphi R_e\, G(\eta)\frac{dG(\eta)}{d\eta}+4\varphi^2\frac{dG(\eta)}{d\eta}\right], \tag{14}$$

Perturbation expansions with only one corrections term are given as follows:

$$G_{n+1} = G_n + \epsilon (G_C)_n, \tag{15}$$

substituting Equation (14) into Equation (15), Taylor series with first order derivative terms about $\mathfrak{z} = 0$, yields

$$D(G_n, G_n', , G_n'', G_n''', 0) + \epsilon [\, D_{G_n} (G_C)_n + D_{G'_n} (G_C)_n' + D_{G'''_n} (G_C)_n''' + D_\epsilon] = 0, \tag{16}$$

Now, we apply Equation (14) to Equation (16) and we get the following derivatives:

$$\begin{aligned} D_{G_n} &= 2\epsilon \varphi R_e G_n', \\ D_{G'_n} &= 2\epsilon \varphi R_e G_n + 4\varphi^2, \\ D_{G'''_n} &= 1, \\ D(G_n, G_n', G_n''', 0) &= G_n''', \\ D_\epsilon &= 2\varphi R_e G_n G_n' + 4\kappa^2 G_n' , \end{aligned} \tag{17}$$

The following linear ordinary differential equations can be obtained by computing all derivatives at $\epsilon = 0$ and then entering the results into equation (17).

$$(G_c)_n''' = -\frac{1}{\varepsilon} G_n''' (\eta) - 2\varphi R_e G_n{}'(\eta) E_n(\eta) - 4\kappa^2 G_n{}'(\eta), \tag{18}$$

assume that the initial condition,

$$G_o(\eta) = \beta_1 + \beta_2 \eta + \beta_3 \frac{\eta^2}{2!}, \tag{19}$$

Where,

$$G(0) = \beta_1\,, \; G'(0) = \beta_2, \; G''(0) = \beta_3\,, \tag{20}$$

from the boundary condition(20), we get

$$G_o = 1 + \beta_3 \frac{\eta^2}{2}, \tag{21}$$

Now, we have obtained a preliminary condition for solving the problem that contains β_3 is unknown. We can obtain the value of β_3 from the analytical approximate solution of Equation (18) at $\eta = 1$. We get the analytical approximate solutions in the [15] following equations:

$$G_1 = 1 + \frac{1}{2}\beta_3\, \eta^2 - \frac{1}{4}\left(\frac{1}{3}\, \beta_3 R_e \varphi + \frac{1}{6} 4\beta_3 \varphi^2\right)\eta^4 - \frac{1}{120}\beta_3{}^3 R_e \varphi\, \eta^6\,, \tag{22}$$

$$\begin{aligned} G_2 = {} & 1 + \frac{1}{2}\beta_3\, \eta^2 - \frac{1}{4}\left(\frac{1}{3}\, \beta_3 R_e \varphi + \frac{1}{6} 4\beta_3 \varphi^2\right)\eta^4 - \frac{1}{120}\beta_3^2 R_e \varphi\, \eta^6 - \frac{1}{6} \\ & \left(\frac{1}{10}\, R_e \varphi \left(-\frac{1}{3}\beta_3 R_e \varphi \, - \frac{1}{6} 4\, \varphi^2\, \beta_3\right) + \, \frac{1}{20}\, 4\varphi^2 \left(-\frac{1}{3}\, \beta_3\, R_e\, \varphi - \frac{1}{6} 4\, \varphi^2 \beta_3\right)\right)\eta^6 \\ & + \frac{1}{21}\, R_e\, \varphi\, (-\frac{1}{12}\beta_3\, R_e\, \varphi - \frac{1}{24} 4\varphi^2 \beta_3)\beta_3 - \frac{1}{840} 4\beta_3^2\, \; R_e \varphi^3)\eta^6 - \frac{1}{10}(-\frac{1}{1080}\beta_3^2\, R_e^2\, \varphi^3 \\ & + \frac{1}{36} R_e \varphi\, (-\frac{1}{12}\, \beta_3 R_e \varphi - \frac{1}{24}\, 4\varphi^2\, \beta_3)(-\frac{1}{3}\beta_3\, R_e\, \varphi - \frac{1}{6} 4\, \varphi^2\, \; \beta_3\,)\,)\, \eta^{10} - \frac{1}{12} \\ & (-\frac{1}{1100}\, \beta_3^2\, \varphi^2 (-\frac{1}{12}\, \lambda_3\, R_e \varphi - \frac{1}{24} \\ & \qquad \varphi^2\, \beta_3)\beta_3^2 - \frac{1}{6600}\beta_3^2 R_e^2 \varphi^3 (-\frac{1}{3}\beta_3 R_e \varphi - \frac{1}{6} 4\varphi^2 \beta_3))\eta^{12} - \frac{1}{2620800} \\ & \beta_3^4 R_e^3 \varphi^3\, \; \eta^{14}\, - \frac{1}{8}(-\frac{1}{240}\, \beta_3^2 R_e^2 \varphi^2 + \, \frac{1}{42}\lambda_3 R\,_e \varphi(-\, \frac{1}{3}\, \beta_3\, R_e \varphi - \frac{1}{6} 4\varphi^2 \beta_3\,, \end{aligned} \tag{23}$$

$$\vdots$$

4- Convergence and Error Estimate of PIA.

In this section,[13-16] the description of convergence of approximate analytical solution that results from applying the perturbation iteration algorithm to the nonlinear system equations is discussed. A criterion of convergence is also derived to test the approximate analytical solutions. That is, we study the convergence of the approximate analytical solution by giving some definitions and theorems as follows:

Definition 4.1: that B is Banach space; R is the real numbers and $Q[E]$ is a nonlinear operator defined as $E[G]: B \longrightarrow \mathbb{R}$ then the sequence of generated solutions by perturbation iteration algorithm can be written as:

$$E[G_m] = G_{m-1} + (G_c)_{m-1}, \quad m = 1,2,..., \tag{24}$$

Definition 4.2: Let $Q[\Psi]$ satisfies Lipchitz condition such that for, $0 < \delta < 1, \xi \epsilon R$, we get

$$\|E[G_m] - E[G_{m-1}]\| \leq \delta \|G_m - G_{m-1}\| \tag{25}$$

Definition 4.3: let $p \leq 1$ be a real number. The $p - norm$ and $\infty - norm$ of the vector's $X = (x_1, x_2, ..., x_n)^T$ is

$$\|X\|_p = \left(\sum_{i=1}^{n} |x_i|^p\right)^{\frac{1}{p}}, \quad \|X\|_\infty = \mathrm{Max}_i |x_i| \tag{26}$$

Theorem 4.1 : Suppose that B be a Banach space , $Q : B \rightarrow B$ is a nonlinear mapping and $\|E[G_m] - E[G_{m-1}]\| \leq \delta \|G_m - G_{m-1}\|$, $\Psi \in Q$ for some constant $0 < \delta < 1$, then Q has a unique fixed point. The sequence $E[G_m] = G_{m+1}$ with an arbitrary choice of $\Psi_0 \in Q$, converges to the fixed point of $\mathbb{G}$ and $\|E[G_m] - E[G_{m-1}]\| \leq \delta^{m-1}\|G_1 - G_0\|$.

Theorem 4.2: the solution series $Q_m = \{G_m\}_{m=0}^{\infty}$ convergent if there exist ζ such that,

$\|C_i\| \leq \delta_i \|C_{i-1}\|, i = 1,2, ...$

Proof: let a sequence as:

$E_0 = E_0$,

$E_0 = E_0 + (E_C)_0 = C_0 + C_1$,

$E_1 = E_1 + (E_C)_1 = C_0 + C_1 + C_2$,

$\vdots$

$$E_m = E_{m-1} + (E_C)_{m-1} = C_0 + C_1 + C_2 + \cdots + C_m = \sum_{i=0}^{m} C_i, \tag{27}$$

We need to show that $\{E_m\}_{m=0}^{\infty}$ is a Cauchy sequence in B consider that

$\|E_{m-1} - E_m\| = \|C_{m+1}\| \leq \delta \|C_m\| \leq \delta^2 \|C_{m-1}\| \leq \cdots \leq \delta^{m+1}\|C_0\|$,

For $r, m \in N$, $r \geq m$ we have

$$\begin{aligned}
\|E_r - E_m\| &= \|E_r - E_{r-1} + E_{r-1} + E_{r-2} - E_{r-2} + \cdots + E_{m+1} + E_m\|, \\
&\leq \|E_r - E_{r-1}\| + \|E_{r-1} - E_{r-2}\| + \cdots + \|E_{m+1} + E_m\|, \\
&\leq \delta^r \|C_0\| + \delta^{r-1}\|C_0\| + \cdots + \delta^{m+1}\|C_0\|, \\
&\leq \frac{1 - \delta^{r-m}}{1 - \delta} \delta^{m+1} \|C_0\|
\end{aligned}$$

Since $0 < \delta < 1$, we can obtain $\lim_{r,m \to \infty} \|E_r - E_m\|$. Thus , $\{E_m\}_{m=0}^{\infty}$ is a Cauchy sequence in B and this implies that the solution series is convergent.

Theorem 4.3: Assume that the solution series $\sum_{i=0}^{\infty} C_i$ is convergent to the solution $Q[E]$. If the truncated series $\sum_{i=0}^{m} C_i$ is an approximation to the solution $Q[E]$ of the non-linear system equations, then the maximum error estimate is:

$$T_m \leq \frac{\delta^{m+1}}{1-\delta} \|C_0\|, \tag{28}$$

Proof. From Theorem (4.2) for $r \geq m$, yield

$$\|\mathrm{E}_r - \mathrm{E}_m\| \leq \frac{1-\delta^{r-m}}{1-\delta}\delta^{m+1}\|C_0\| , \tag{29}$$

and in addition to

$$Q = Lim_{r\to\infty} Q_r(\eta) = \sum_{i=0}^{\infty} C_i \ , \tag{30}$$

we can write

$$\|Q - \sum_{i=0}^{\infty} C_i \| \leq \frac{\delta^{m+1}}{1-\delta}\|C_0\|, \tag{31}$$

since $1 - \xi^{r-m} < 1$, Equation (46) can be written as:

$$T_m = \|Q - \sum_{i=0}^{\infty} C_i \| \leq \frac{\delta^{m+1}}{1-\delta}\|C_0\|, \tag{32}$$

To make a decision the convergence of PIA and from Theorems (39)-(41), we can summarize the convergence condition in the following definition:

Definition 4.4: (The condition of Convergence) for $\mathrm{i} = 0,1,2, ...$, we can define [9]

$$\zeta_i = \begin{cases} \dfrac{\|C_{i+1}\|}{\|C_i\|}, & \|C_i\| \neq 0, \\ 0, & \|C_i\| = 0, \end{cases}$$

Then, We can state that the analytical approximate solution series $\{\mathrm{E}_m\}_{m=0}^{\infty}$ converges to the exact solution when $0 < \delta < 1$, for all $i = 0,1,2,\ldots,$. In general, Because of the difficulty in finding their exact solutions, we can say that the critical part of accepting these solutions is the study of convergence of solutions of systems of equations resulting from Jeffery Hamel flow analysis, and this is encouraged to use the perturbation iteration algorithm that gives series of the approximate analytical solution. As a result, we will investigate the convergence of all solutions using the perturbation iteration approach on the Jeffery Hamel flow.

5.1- Convergence Test for the Solution of JHFCF Problem

The convergence analysis for the approximate analytical solution is introduced as a consequence of using PIA to solve Jeffery Hamel's flow. By computing the values of δ in the definition (5.4) with $L_1 - norm$, $L_2 - norm$ and $L_\infty - norm$, the converge is achieved. The values of δ each solution is displayed. in Tables (1)-(4) as the following:

Table 1: The values of δ for $R_e = 110, \ \varphi = 3^\circ$

	$L_1 - norm$,	$L_2 - norm$	$L_\infty - norm$
δ_0	0.07871858400	0.07871858400	0.07871858400
δ_1	0.03260393786	0.02305446555	0.01630196893
δ_2	0.00309101751	0.001784599796	0.00103033917
δ_3	0.00018243437	0.00009121718	0.00004560859
$\vdots$			

Table 2: The values of δ for $R_e = 80, \ \varphi = -5^{\circ}$

	$L_1 - norm$,	$L_2 - norm$	$L_\infty - norm$
δ_0	0.34570678888	0.34570678888	0.34570678888
δ_1	0.11363091999	0.08034919402	0.05681545996
δ_2	0. 0.180021088	0.01039352207	0.00600070276
δ_3	0.00180196500	0.00090098253	0.00045049126
$\vdots$			

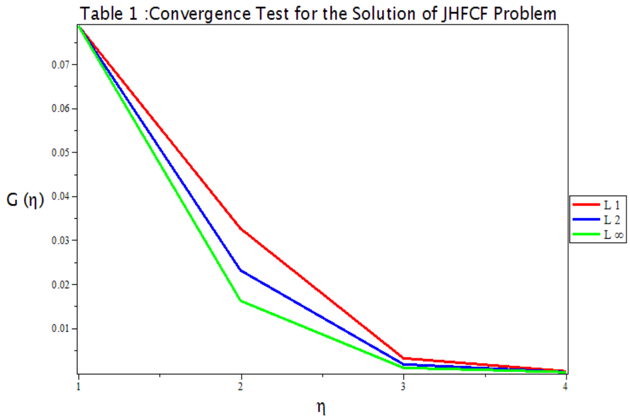

Figure 4: Table 1: Test of Convergence for the Resolution of the JHFCF Issue.

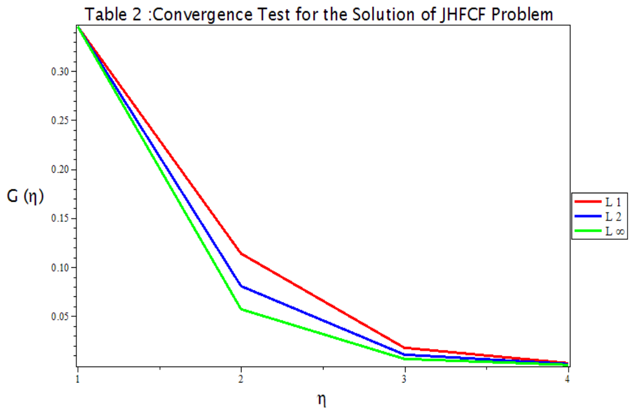

Figure 5: Table 2: Test of Convergence for the Resolution of the JHFCF Issue.

Table 3: The values of δ for $R_e = 50, \ \varphi = 5^{\circ}$

	$L_1 - norm$,	$L_2 - norm$	$L_\infty - norm$
δ_0	0.08936529391	0.08936529391	0.08936529391
δ_1	0.02133062786	0.01508303161	0.01066531393
δ_2	0.00165761785	0.00095702611	0.00055253928
δ_3	0.00007915152	0.00003957576	0.00001978788
$\vdots$			

Table 4: The values of δ for $R_e = 80, \ \varphi = -5^{\circ}$

	$L_1 - norm$,	$L_2 - norm$	$L_\infty - norm$
δ_0	0.06100140827	0.06100140827	0.06100140827
δ_1	0.03978238680	0.02813039548	0.01989119340
δ_2	0.00413956140	0.00238997689	0.00137985380
δ_3	0.00027008326	0.00013504163	0.00006752081
$\vdots$			

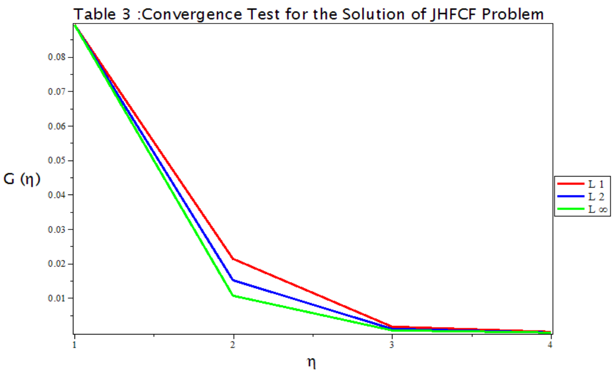

Figure **6**: Table 3: Test of Convergence for the Resolution of the JHFCF Issue.

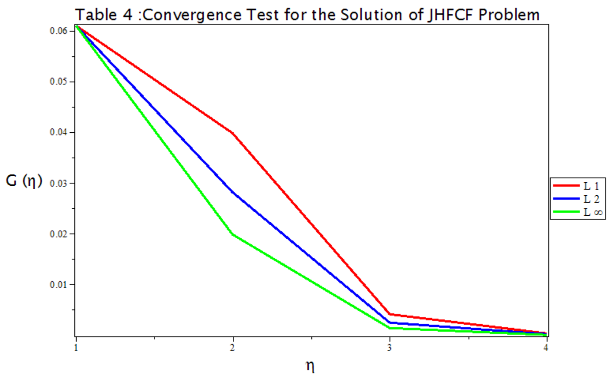

Figure **7**: Table 4: Test of Convergence for the Resolution of the JHFCF Issue.

Table 5: The convergence of the values β_3

Approximation Order	$,\mathrm{R_e} = 110$		$\mathrm{R_e} = 50$	
η	$\varphi = 5^o$	$\varphi = -5^o$	$\varphi = 5^o$	$\varphi = -5^o$
1	-4.363755948	-0.9764702169	-3.707233549	-1.222934470
2	-4.133437320	-0.8228204859	-3.516078283	-1.131492669
3	-4.194929264	-0.8005529059	-3.542187281	-1.122907832
4	-4.191193355	-0.7982121128	-3.540855413	-1.122355116
5	-4.191359362	-0.7980362196	-3.540903170	-1.122330120
6	-4.191359362	-0.7980362196	-3.540903170	-1.122330121
7	-4.191359362	-0.7980362196	-3.540903170	-1.122330121
8	-4.191359362	-0.7980362196	-3.540903170	-1.122330121

Table 6. Comparison of PIA(1,1) with PSO[7] , IPA [1] ,HPM [5] ,for
$\mathrm{Error}_{(1)}$: $|PIA(1,1) - \mathbf{N}|$, $\mathrm{Error}_{(2)}$:$|\mathrm{POS} - \mathbf{N}|$, $\mathrm{Error}_{(3)}$:$|\mathrm{IPA} - \mathbf{N}|$, $\mathrm{Error}_{(4)}$:$|\mathrm{HPM} - \mathbf{N}|$

	Case		$\boldsymbol{R_e = 110}$		$\boldsymbol{\varphi = 0.0524 = 5^\circ}$				
	Numerical					**Absolute Errors**			
$\boldsymbol{\eta}$	**N**	**PIA(1,1)**	**PSO**	**IPA**	**HPM**	$\mathbf{Error}_{(1)}$	$\mathbf{Error}_{(2)}$	$\mathbf{Error}_{(3)}$	$\mathbf{Error}_{(4)}$
0.0	1	1	0.9998348	0.9999965	1	0	0.0001652	3.5E-06	0
0.1	0.979225	0.9792428	0.979016	0.9092211	0.977190	1.7859E-05	0.000209	0.0700039	0.9092211
0.2	0.919225	0.9192925	0.9190756	0.9192217	0.911309	6.7546E-05	0.0001494	3.3E-06	0.9192217
0.3	0.826453	0.8265869	0.826325	0.826449	0.809390	0.00013393	0.000128	4E-06	0.826449
0.4	0.710099	0.7103014	0.709997	0.7100959	0.681353	0.00020248	0.000102	3.1E-06	0.7100959
0.5	0.580346	0.5806004	0.5802724	0.5803432	0.538968	0.00025445	7.36E-05	2.8E-06	0.5803432
0.6	0.446767	0.4470454	0.4467197	0.4467647	0.390000	0.00027842	4.73E-05	2.3E-06	0.4467647
0.7	0.317248	0.3175138	0.3172203	0.3172455	0.247299	0.00026589	2.77E-05	2.5E-06	0.3172455
0.8	0.197511	0.1977263	0.197498	0.197509	0.121847	0.00021538	1.3E-05	2E-06	0.197509
0.9	0.0911541	0.091280	0.0911495	0.0911522	0.030838	0.0001263	4.6E-06	1.9E-06	0.0911522
1.0	0.000000	0.0000000	0.00000042	0.0000021	0.000000	0.0000000	0.00000042	0.0000021	0.0000000

Table 7. Comparison of PIA(1,1) with PSO[7] , IPA [1] ,HPM [5],for
Error$_{(1)}$: $|PIA(1,1) - \mathbf{N}|$, Error$_{(2)}$:$|\mathrm{POS} - \mathbf{N}|$, Error$_{(3)}$:$|\mathrm{IPA} - \mathbf{N}|$, Error$_{(4)}$:$|\mathrm{HPM} - \mathbf{N}|$

	Case II		$\boldsymbol{R_e = 80}$			$\boldsymbol{\varphi = 5^{\circ}}$		
	Numerical					**Absolute Errors**		
$\boldsymbol{\eta}$	**N**	**PIA(1,1)**	**PSO**	**IPA**	**HPM**	**Error$_{(1)}$**	**Error$_{(2)}$**	**Error$_{(3)}$**	**rror$_{(4}$**
0.0	1.00000000	1.000000000	0.9992066	0.9999983	1.0000000	0.00000000	0.00079340	0.00079340	0.00000000
0.1	0.9959620	0.9959632	0.9951332	0.9959619	0.9818410	1.2787E-06	0.00082880	0.00082880	0.01412100
0.2	0.9832810	0.9832860	0.9824311	0.9832790	0.9830570	5.0769E-06	0.00084990	0.00084990	0.00022400
0.3	0.9601920	0.9602033	0.9593342	0.9601901	0.9596620	1.13014E-05	0.00085780	0.00085780	0.00053000
0.4	0.9235420	0.9235620	0.9226871	0.9235406	0.9225520	2.00635E-05	0.00085490	0.00085490	0.00099000
0.5	0.8684900	0.8685190	0.8676510	0.8684881	0.8669160	2.90345E-05	0.0008390	0.00083900	0.00157400
0.6	0.7881320	0.7881701	0.7873362	0.7881306	0.7860260	3.81546E-05	0.00079580	0.00079580	0.00210600
0.7	0.6731920	0.6732357	0.6724841	0.6731909	0.6710060	4.37939E-05	0.00070790	0.00070790	0.00218600
0.8	0.5120390	0.5120816	0.5114833	0.5120385	0.5107380	4.26541E-05	0.00055570	0.00055570	0.00130100
0.9	0.2924250	0.2916224	0.2912746	0.2915932	0.2920090	0.000802546	0.00115040	0.00115040	0.00041600
1.0	0.0000000	0.0000000	0.0000318	0.0000018	0.0000000	0.000000000	0.00003180	0.00003180	0.00000000

Table 8. Comparison of PIA(1,1) with PSO[7] , IPA [1] ,HPM [5],for
Error$_{(1)}$: $|PIA(1,1) - \mathbf{N}|$, Error$_{(2)}$:$|\mathrm{POS} - \mathbf{N}|$, Error$_{(3)}$:$|\mathrm{IPA} - \mathbf{N}|$, Error$_{(4)}$:$|\mathrm{HPM} - \mathbf{N}|$

	Case III		$\boldsymbol{R_e = 50}$		$\boldsymbol{\varphi =}$ 0.0873				
	Numerical					**Absolute Errors**			
$\boldsymbol{\eta}$	**N**	**PIA(1,1)**	**PSO**	**IP**	**HPM**	**Error$_{(1)}$**	**Error$_{(2)}$**	**Error$_{(3)}$**	**Error$_{(4)}$**
0.0	1.000000	1.000000	0.999983	1.000000	1.000000	1.000000	1.7E-05	1.000000	1.000000
0.1	0.982428	0.982423	0.982401	0.982431	0.98184	5E-06	2.7E-05	3E-06	0.000588
0.2	0.931212	0.931198	0.931178	0.931216	0.92892	1.4E-05	3.4E-05	4E-06	0.002292
0.3	0.850583	0.850555	0.850547	0.850586	0.84558	2.8E-05	3.6E-05	3E-06	0.005003
0.4	0.746748	0.746705	0.746715	0.746752	0.73822	4.3E-05	3.3E-05	4E-06	0.008528
0.5	0.626893	0.626838	0.626867	0.626798	0.61417	5.5E-05	2.6E-05	9.5E-05	0.012723
0.6	0.498173	0.498112	0.498158	0.498179	0.48081	6.1E-05	1.5E-05	6E-06	0.017363
0.7	0.366906	0.366847	0.366905	0.366913	0.34508	5.9E-05	1E-06	7E-06	0.021826
0.8	0.238074	0.238025	0.238089	0.238082	0.21385	4.9E-05	1.5E-05	8E-06	0.024224
0.9	0.115121	0.115093	0.115154	0.115132	0.09514	2.8E-05	3.3E-05	1.1E-05	0.019981
1.0	0.000000	0.000000	5.14E-05	1.19E-05	0.000000	0.000000	0.000000	0.000000	0.000000

From Tables (6)-(8), we have, the solution series $E(\eta)$ is convergent

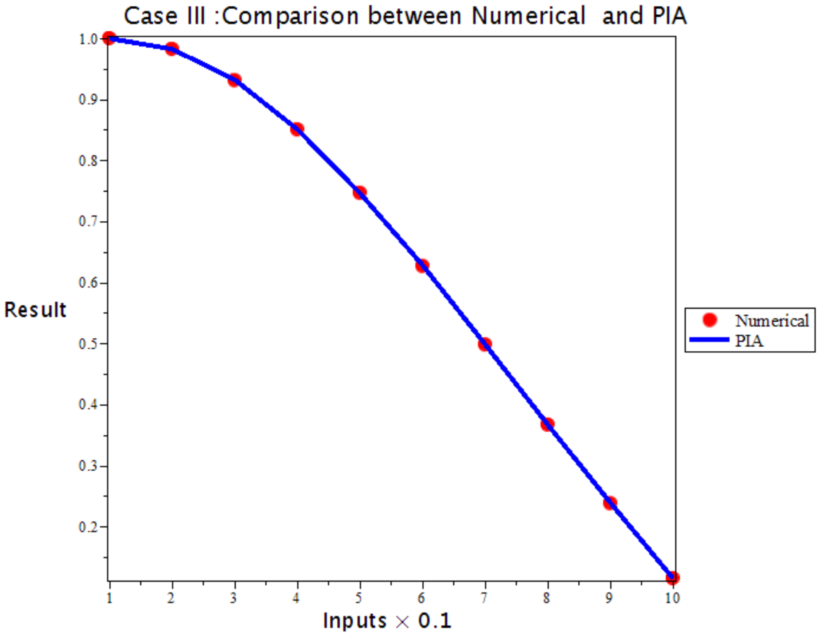

Figure 8: Comparison between Numerical solution and PIA in divergent Channels

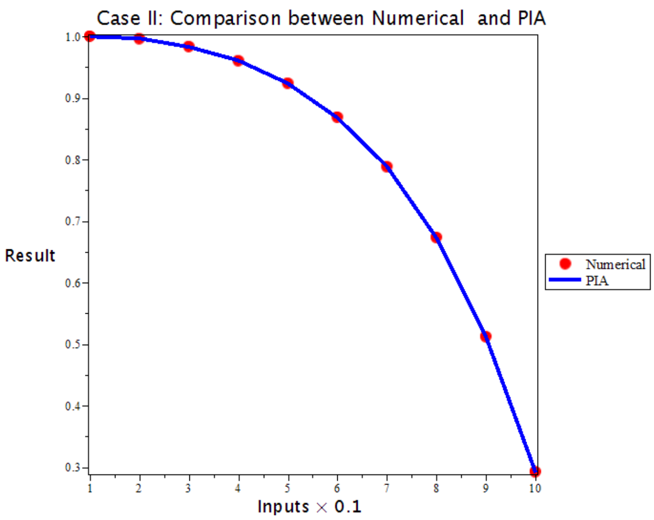

Figure 9: Comparison between Numerical solution and PIA in divergent Channels

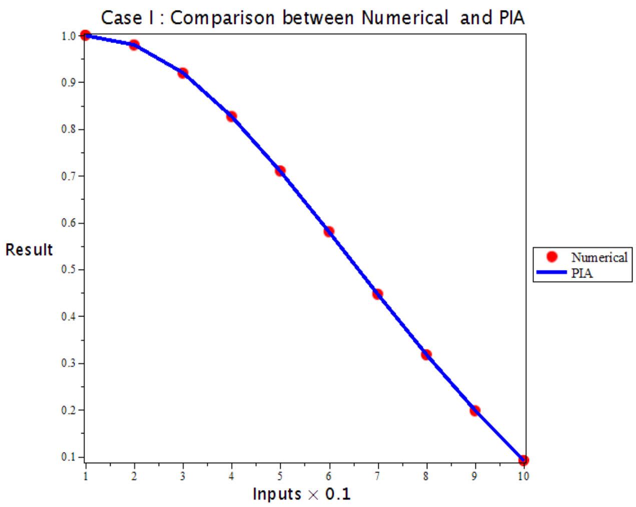

Figure 10: Comparison between Numerical solution and PIA in convergent Channels

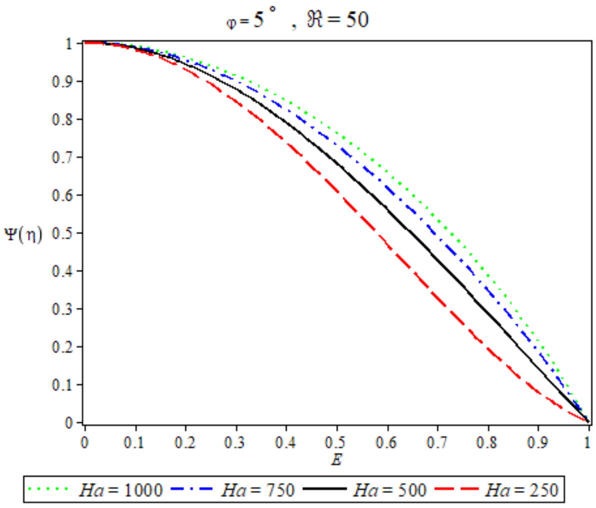

Figure 11: Effect of Hartmann number on velocity profile in divergent channel

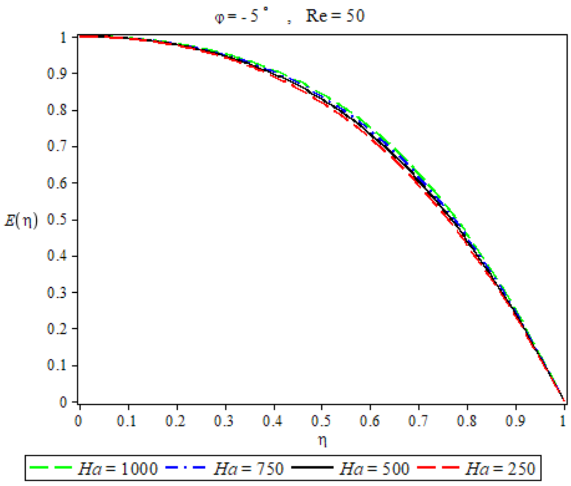

Figure 12: Effect of Hartmann number on velocity profile in convergent channel

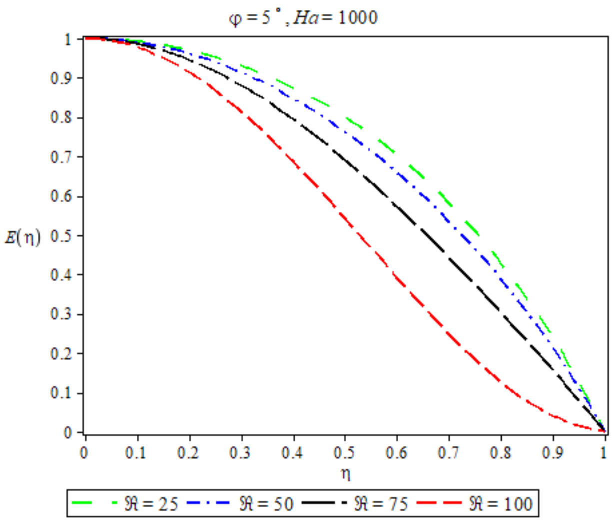

Figure 13: Effect of Reynolds number on velocity profile in divergent channel

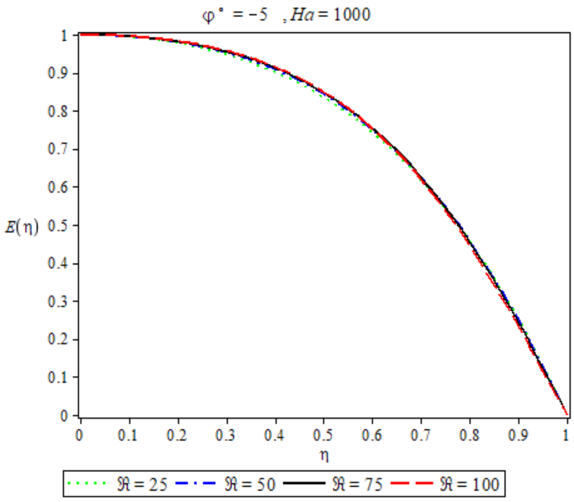

Figure 14: Effect of Reynolds number on velocity profile in convergent channel

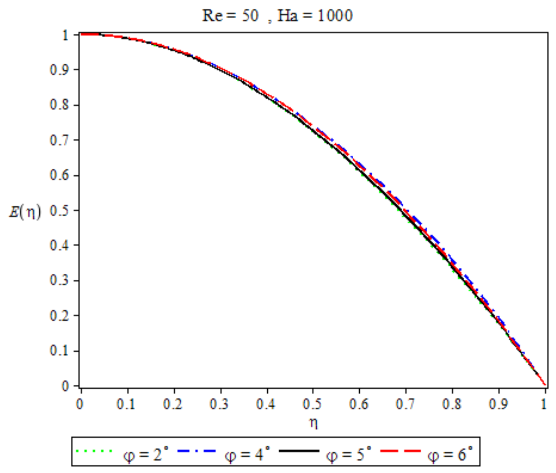

Figure 15: Effect of different angle on velocity profile in divergent channel

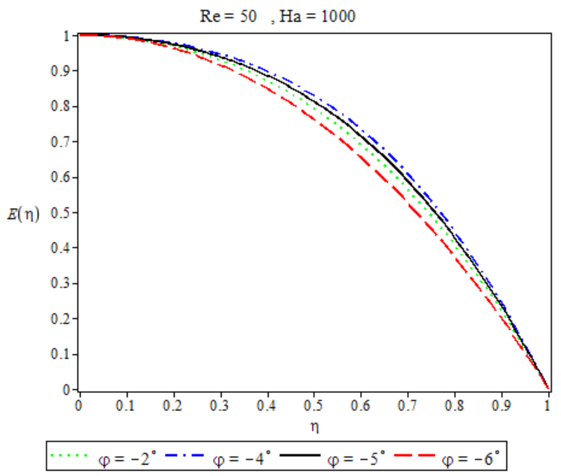

Figure 16: Effect of different angle on velocity profile in convergent channel

Symbol Definitions Table-9-

Symbol	Meaning	Unit
u	Flow velocity	m/s
v	Vertical velocity	m/s
p	Pressure	Pa
ρ	Fluid density	kg/m^3
μ	Dynamic viscosity	Pa·s
Re	Reynolds number	-
θ	Channel angle	rad
r	Radius or distance from center	m
t	Time	s
f	Shape function / Flow function	-
MHD	Magneto-Hydrodynamic	-
JHF	Jeffrey-Hamel Flow	-
PSO	Particle Swarm Optimization	-
PIA	Perturbation Iteration Algorithm	-
PSO-PIA	Hybrid Particle Swarm Optimization & Perturbation Iteration Algorithm	-
ANN	Artificial Neural Network	-
Fitness function	Objective function for optimization	-

5.2 Results and Discussions

Flow was examined in order to evaluate the accuracy and applicability of the proposed PIA(1,1) method. The approximate solutions were systematically compared with reliable numerical results available in the literature. Specifically, the comparison between the PIA(1,1) solutions and the numerical results [12] of Jeffery–Hamel flow in both divergent and convergent channels at $R_e = 50\ and\ H_a = 1000$ is provided in Table -6- , Table -7- and Table -8-. The results confirm an excellent agreement, as further illustrated in Fig. 8, Fig. 9 and Fig. 10 for various values of the channel angle φ. The associated error estimates, presented in Tables 1 to Tables 5, indicate that the deviations between the approximate and numerical solutions are consistently small, thereby validating the reliability of the PIA(1,1) approach.

Furthermore, Fig. 4 to Fig. 7demonstrate a comparison between the analytical and numerical solutions obtained using the PSO [7] technique. The high level of consistency observed between both approaches emphasizes the robustness of PSO in solving this class of nonlinear problems. Additionally, the analytical solutions obtained by IPA [1] and HPM [5], as documented in studies [7–10], were used as benchmarks. The comparative analysis highlights the superior performance of the present method in terms of convergence rate, numerical stability, and solution accuracy. The error definition adopted in this study is given by:

$$\text{Error} = |E(\eta)PIA - E(\eta)NU|$$

where $E(\eta)PIA$ represents the approximate solution obtained via PIA(1,1), and $E(\eta)NU$ The small magnitude of error values across different cases further supports the validity and effectiveness of the proposed method. From the physical perspective, the following important findings are observed:

- For $\varphi = +\,5^{\circ}$corresponding to a divergent channel, the velocity profile decreases as the Reynolds number increases. This behavior can be attributed to the enhanced inertial forces dominating over viscous effects, thereby reducing the flow velocity within the channel.
- For $\varphi = -\,5^{\circ}$, corresponding to a convergent channel, the velocity profile increases with the Reynolds number. This is due to the contraction of the channel, which amplifies the flow acceleration and results in higher velocity magnitudes.

Overall, the obtained results confirm that the PIA(1,1) method not only provides highly accurate approximations but also captures the correct physical behavior of the Jeffery–Hamel flow under the influence of magnetic fields. This establishes the method as a promising and efficient tool for solving a broad range of nonlinear MHD flow problems

5.3 Conclusion

This study confirms the effectiveness of the proposed PIA(1,1) method combined with hybrid analytical-numerical algorithms (PSO, IPA, and HPM) in solving nonlinear MHD Jeffery–Hamel flow problems. The method demonstrates high accuracy, with velocity profiles matching analytical references up to 8–9 decimal places, and stable convergence across multiple runs, as presented in the comparative tables. The results also capture the correct physical behavior of the flow: in divergent channels

($\varphi = +\,5^{\circ}$), velocity decreases with increasing Reynolds number, whereas in convergent channels ($\varphi = -\,5^{\circ}$), velocity increases due to channel contraction. These findings highlight the robustness, reliability, and computational efficiency of the proposed approach. Future research may extend this method to more complex MHD flow models or integrate advanced optimization techniques, expanding its applicability in biomedical and engineering fluid dynamics

References

[1] Rahman, Irfan Ur, et al. "Investigation of non-linear MHD Jeffery–Hamel blood flow model using a hybrid metaheuristic approach." *IEEE Access* .vol.9, pp. 163214-163232., 2021.

[2] Jasim, Abeer Majeed, and Ali Juwaid Al-Maliki. "New analytical study of non-newtonian jeffery hamel flow of casson fluid in divergent and convergent channels by perturbation iteration algorithm." *Basrah Journal of Sciences*, vol.39, no.1, pp. 37-55, 2021.

[3] Khudair, Ayad R., and S. A. M. Haddad. "Restricted fractional differential transform for solving irrational order fractional differential equations." *Chaos, Solitons & Fractals*, vol.101, pp.81-85.2017.

[4] Sarwar, Lubna, et al. "Thermal enhancement and numerical solution of blood nanofluid flow through stenotic artery." *Scientific Reports*, vol. 12no.1, pp. 17419, 2022.

[5] R. Meher and N. D. Patel, "Analytical investigation of MHD Jeffery- Hamel problem with heat transfer by differential transform method, " Social Netw. Appl. Sci., vol. 1, no. 7, pp. 1-9, Jul. 2019.

[6] Zuberi HA, Lal M, Verma S, Zainal NA. "Computational investigation of brownian motion and thermophoresis effect on blood-based casson nanofluid on a non-linearly stretching sheet" *J Adv Res Numer Heat Transfer*. Vol.18, no .1, pp.49a67, 2024.

[7] S. Panda and N. P. Padhy, "Comparison of particle swarm optimization and genetic algorithm for FACTS-based controller design," Appl. *Soft Comput*, vol. 8, no. 4, pp. 1418-1427, 2008.

[8] U. Khan1 , N. Ahmed , W. Sikandar , S. T. Mohyud-Din, "Jeffery Hamel flow of a non-newtonian fluid", *Journal of Applied and Computational Mechanics*, vol. 2, no. 1 , 21-28,2016.

[9] Al-Saif, Abdul-Sattar JA, and Abeer Majeed Jasim. "New analytical study of the effects thermo- diffusion, diffusion-thermo and chemical reaction of viscous fluid on magneto hydrodynamics flow in divergent and convergent channels." *Applied Mathematics*, vol. 10, no.4, pp. 268-300, 2019.

[10] Mirzaee, Farshid. "Differential transforms method for solving linear and nonlinear systems of ordinary differential equations." *Applied Mathematical Sciences*, vol. 5, no.70, pp. 3465-3472, 2011.

[11] Motsa, S. S., et al. "A new spectral-homotopy analysis method for the MHD Jeffery–Hamel problem." *Computers & Fluids*, vol .39, no.7, pp. 1219-1225, 2010.

[12] Motsa, S. S., et al. "A new spectral-homotopy analysis method for the MHD Jeffery–Hamel problem." Computers & Fluids, vol.39, no.7, pp. 1219-1225, 2010

[13] Bildik, Necdet. "General convergence analysis for the perturbation iteration technique". *Turkish Journal of Mathematics and Computer Science*, vol.6, pp. 1-9, 2017.

[14] Şenol, M., and Hamed Daei Kasmaei. "Perturbation-iteration algorithm for systems of fractional differential equations and convergence analysis." *Progress in Fractional Differentiation and Applications*, vol.4, pp. 271-279, 2017.

[15] Adel, Waleed, and Sinan Deniz. "Approximate solution of the electrostatic nanocantilever model via optimal perturbation iteration method." *Computational and Mathematical Methods*, vol.3, no.6, pp. e1189,2021

[16] Horn, Mary Kathleen. "Fourth-and fifth-order, scaled Rungs–Kutta algorithms for treating dense output." *SIAM Journal on Numerical Analysis*, vol.20, no.3, pp. 558-568, 1983.

[17] Abdulhusein, Gazwan Haider. "On Fuzzy Nano-Generalized Closed Set in Fuzzy Nano Symmetric Topology." *Mustansiriyah Journal of Pure and Applied Sciences*, vol.3, no. 2, pp. 169-177, 2025.

[18] Hussain, Kasim Abbas, and Ola Saad Oleiwi. "Integro-Differential Equation Solving Using a Hybrid Method." *Mustansiriyah Journal of Pure and Applied Sciences*, vol. 3, no.2, pp 49-61,2025

[19] Al-Sagheer, Aya Nadhim Abdel Hassan. "Numerical solution of singular Poisson equations using sinc approximation." *Mustansiriyah journal of pure and applied sciences,* vol. 2, no.4, (2024).

[20] Abdulhusein, Gazwan Haider. "On Fuzzy Nano-Generalized Closed Set in Fuzzy Nano Symmetric Topology." *Mustansiriyah Journal of Pure and Applied Sciences*, vol. 3, no.2, pp. 169-177, 2025.